Modeling hydrodynamics and biochemical reactions in a Flat Plate Bioreactor

Ll. Prades [1], X. Guimerà [1], J. Climent [2], S. Chiva [2], A. D. Dorado [1], X. Gamisans [1]
[1] Department of Mining Engineering and Natural Resources, Universitat Politècnica de Catalunya, Bases de Manresa 61-73, 08240 Manresa, Spain
[2] Department of Mechanical Engineering and Construction, Universitat Jaume I, Avd. Vicent Sos Baynat s/n, 12071 Castelló de la Plana, Spain.
e-mail: lledo.prades@emrn.upc.edu

Abstract
Modeling the complex interactions between biochemical reactions and hydrodynamics is the key to optimize biofiltration systems performance. In this work, biological kinetics expressions were implemented into Computational Fluid Dynamics (CFD) model as transport equations, including convective and diffusive terms. Previously, activity within the biofilm of a flat plate bioreactor (FPB) was experimentally investigated measuring dissolved oxygen (DO) profiles by means of microsensors and under common operating conditions. Moreover, a mathematical model to describe mass transport and metabolic activity in the FPB was developed and their parameters were fitted from experimental results. Then, a CFD model, combining hydrodynamics and biochemical reactions, was developed and solved to simulate local transient flow and dynamic behaviors of biofilm growth and substrate (glucose) biodregradation in the FPB. The CFD simulation results were evaluated by studying hydrodynamics characterization in the FPB and comparing simulated DO profiles with experimental DO profiles within the biofilm section. The hydraulic behaviour corresponds to a laminar flow and simulated DO profiles illustrate a satisfactory agreement with experimental data for different biofilm densities. Glucose and oxygen biodegradation and biomass growth along the bioreactor were described using the CFD model.

Keywords
CFD; Modeling; Flat plate bioreactor; Biochemical reactions; Hydrodynamics; Dissolved oxygen;

INTRODUCTION

Biotrickling filters have been successfully implemented in the abatement of a large amount of gaseous pollutants (Iranpour et al., 2005). These techniques are based on the use of the metabolic diversity of microorganisms to degrade, transform or accumulate a wide range of compounds. For this reason, microorganisms are an essential element in bioreactors operation, where they grow as a fixed film, while interacting with their environment through the liquid phase that flows over them. This fluid flow influences biofilm development and activity by the transport of dissolved solutes into and out of the biofilm, and the application of shear forces to the biofilm (Stewart, 2012). However, a detailed knowledge of these very complex multiphase systems, involving coupling of two-phase fluid flow, interfacial mass transfer, and intrinsic bioreaction, is rather limited.

Several mathematical models of biofilms have been developed, from the first-generation of models, which describe mass flux and concentration profiles within the biofilm using one-dimensional geometry, until the third-generation, in which all components can vary in multi-dimensional space, as well as time, so they can generate complex physical and ecological structures (IWA Task Group on Biofilm Modeling, 2006). In this third-generation of models, different works have been developed to evaluate the influence of the liquid flow on the biofilm (Picioreanu et al. 2000, 2001; Taherzadeh et al., 2010). In addition, Computational Fluid Dynamics (CFD) techniques have been employed as a useful tool for understanding multiphase hydrodynamics and biochemical reactions of airlift loop reactors (Feng et al., 2007; Jia et al., 2009; Wang et al., 2011) and activated sludge reactors (Climent et al., 2014; Liotta et al., 2014), where the bioreaction behavior is associated to the liquid phase dynamics. Nevertheless, the complicated interaction of hydrodynamics with mass transfer and bioreaction between the biofilm and liquid phase has not been described using this type of techniques.

Therefore, the aim of this work was to use CFD techniques to model the behaviour of biofilm and liquid phase, considering interphase mass transfer for different species in a bioreactor. For this purpose, previous to develop the CFD model, it was necessary to study the degradation phenomena taking place within the biofilm. A microsensor was used to record experimental DO profiles inside the biofilm. In addition, a dynamic mathematical model was developed, based on mass transport and biological reaction inside the bioreactor. Then, the model parameters were fitted from the experimental results and biological kinetic models were implemented into the CFD code. The developed CFD model may be used to predict hydrodynamics and biodegradation behaviour inside the bioreactor.

MATERIALS AND METHODS

Experimental setup

Experimental measurements were conducted through an aerobic heterotrophic biofilm grown on a flat plate bioreactor (FPB), manufactured in accordance with Lewandowski and Beyenal (2007). The

FPB was launched and operated as described in Guimerà et al. (2015). During DO profiles recording, operating conditions were set up reproducing the operating conditions of a conventional biotrickling filter (flow rate and residence time were adjusted to approximately 1 m h^{-1} and 12 hours respectively).

In the FPB, DO profiles were recorded using a commercial Clark-type microsensor (OX-25, Unisense, Denmark). The electrodes were connected to a 4-channel amplifier (MicrosensorMultimeter, Unisense, Denmark) and polarized at -0.80V (vs Ag/AgCl). Data acquisition was performed using data acquisition software (Sensor Trace Basic, Unisense, Denmark) which resulted in a display of the oxygen profiles in real time on a computer. Linear two-point calibrations, in the measurement medium solution, were performed. Oxygen saturation conditions, taking into account salinity and temperature, were achieved aerating solutions with standard air (21% O_2). In addition, anaerobic conditions were obtained adding Na_2SO_3 to the solution. The sensor positioning within the biofilm was possible through the use of a three-dimensional micromanipulator (MM33-2, Unisense, Denmark), with a precision in z-axis of 10 µm, and in x-/y-axis of 100 µm. The profiles were obtained at different positions along the biofilm and were recorded during substrate consumption conditions. Biofilm density was measured along the reactor, using protein analysis (Bradford, 1976), thus linking experimental profiles with the biofilm density of the section where were recorded. Finally, glucose concentration was measured through the reactor using a refractometer (Refracto 30GS, Mettler Toledo, Switzerland).

Mathematical modeling

The model presented was built coupling the description of the physical transport and the biological processes occurring along the FPB. The theoretical model describing the aerobic glucose biodegradation in the FPB is based on mass balances in the liquid and within biofilm. The assumptions made during the model development, based on consolidate models (Dorado et al., 2008; Kim & Deshusses, 2003), are listed below: (1) The biofilm is uniform in thickness around the reactor. (2) The biofilm is covered by a constant thickness film of liquid. (3) Mass transport throughout the liquid phase is modeled as a sequence of single continuous stirred tank reactors (CSTR's), where each of these reactors has an additional output to the biofilm phase. (4) Mass transport from the liquid phase to the biofilm and throughout the biofilm occurs by diffusion, following Fick's law. (5) No reaction is considered in the liquid phase (there is a negligible amount of biomass in the liquid phase). (6) Degradation within the biofilm is described by Monod equation considering oxygen limitation.

The values of the different parameters used in the FPB model are shown in Table 1.

Table 1. Main parameters of the bioreactor model.

Parameter	Symbol	Value	Units	Reference
Glucose diffusivity in liquid phase	D_{LG}	$6.73 \cdot 10^{-6}$	$cm^2\ s^{-1}$	(Perry & Green, 1997)
O_2 diffusivity in liquid phase	D_{LO}	$1.88 \cdot 10^{-5}$	$cm^2\ s^{-1}$	(Nguyen et al, 2014)
Glucose diffusivity in biofilm phase	D_{BG}	$0.5 \cdot D_{LG}$	$cm^2\ s^{-1}$	(Guimerà et al., 2015)
O_2 diffusivity in biofilm phase	D_{BO}	$0.5 \cdot D_{LO}$	$cm^2\ s^{-1}$	(Guimerà et al., 2015)
Maximum specific growth rate	μ_{max}	$3.92 \cdot 10^{-6}$	s^{-1}	(Guimerà et al., 2015)
Monod half-saturation coefficient for O_2	$K_{S,O}$	0.504	$mg\ L^{-1}$	(Guimerà et al., 2015)
Maintenance factor for O_2	k_d	$1.49 \cdot 10^{-4}$	s^{-1}	(Guimerà et al., 2015)
O_2-biomass yield	$Y_{X/O}$	1.45	-	Experimentally determined
Glucose-biomass yield	$Y_{X/G}$	0.446	-	Experimentally determined

Mass balance for the liquid phase.

Variables considered in the liquid phase are oxygen and glucose. In this phase, the dynamic mass balance for a compound *n*, C_Ln, in a segment *i* is expressed by following equations. Equation 1 is for the first segment (i=1), which bear boundary constraints, and Equation 2 is from the second segment (i=2) to the last bioreactor segment (i=nvs).

$$\left(\frac{V_L}{n_L}\right)\cdot\left.\frac{dC_Ln(i)}{dt}\right|_{i=1} = \left[Q_{rec}+Q_{in}\right]\cdot\left(C_Ln0 - C_Ln(i)\right) - \frac{D_{Ln}\cdot A_c}{FTL\cdot n_L}\cdot\left(C_Ln(i) - C_Bn(i,1)\right) \quad (1)$$

$$\left(\frac{V_L}{n_L}\right)\cdot\left.\frac{dC_Ln(i)}{dt}\right|_{i=2}^{i=nvs} = \left[Q_{rec}+Q_{in}\right]\cdot\left(C_Ln(i-1) - C_Ln(i)\right) - \frac{D_{Ln}\cdot A_c}{FTL\cdot n_L}\cdot\left(C_Ln(i) - C_Bn(i,1)\right) \quad (2)$$

where V_L is the liquid phase volume in L; n_L is the number of divisions in liquid phase; C_Ln is the concentration of n compound in the liquid phase in mg L^{-1}; Q_{rec} is the volumetric flow rate in the recirculation line in L s^{-1}; Q_{in} is the volumetric flow rate in the inlet bioreactor in L s^{-1}; C_Ln0 is the concentration of n compound in the inlet liquid phase in mg L^{-1}; D_{Ln} is the diffusion coefficient of n

compound in liquid phase in $cm^2\ s^{-1}$; A_c is the available surface area between biofilm and liquid phase in cm^2; FTL is the liquid phase thickness in cm; C_Bn is the concentration of n compound in the biofilm in mg L^{-1}.

Mass balance for the biofilm.

In the biofilm phase, the same compounds as in the liquid phase were considered. The dynamic mass balance for a compound *n*, C_Bn, in a segment *i* of the liquid phase and in the *j* layer of the biofilm depth is expressed by Equation 4, except for the first layer near the interface (j=1) and the last before the substratum (j=nb), which bear boundary constraints, and it is expressed in Equations 3 and 5 respectively.

$$\left.\frac{dC_Bn(i)}{dt}\right|_{\substack{i=1\\ j=2}}^{\substack{i=nvs\\ j=nb-2}} = \frac{D_{Ln}}{FTL^2}\cdot\left(C_Ln(i)-C_Bn(i,j)\right)-\frac{D_{Bn}}{\left(FTB/nB\right)^2}\cdot\left(C_Bn(i,j)-C_Bn(i,j+1)\right)+R_Bn(i,j) \quad (3)$$

$$\left.\frac{dC_Bn(i)}{dt}\right|_{i=1}^{\substack{i=nvs\\ j=1}} = \frac{D_{Bn}}{\left(FTB/nB\right)^2}\cdot\left(C_Bn(i,j-1)-2\cdot C_Bn(i,j)+C_Bn(i,j+1)\right)+R_Bn(i,j) \quad (4)$$

$$\left.\frac{dC_Bn(i)}{dt}\right|_{i=1}^{\substack{i=nvs\\ j=nb}} = \frac{D_{Bn}}{\left(FTB/nB\right)^2}\cdot\left(C_Bn(i,j-1)-C_Bn(i,j)\right)+R_Bn(i,j) \quad (5)$$

where C_Bn is the concentration of n compound in the biofilm phase in mg L^{-1}; D_Ln is the diffusion coefficient of n compound in liquid phase in $cm^2\ s^{-1}$; FTL is the liquid phase thickness in cm; C_Ln is the concentration of n compound in the liquid phase in mg L^{-1}; D_{Bn} is the diffusion coefficient of n compound in biofilm phase in $cm^2\ s^{-1}$; FTB is the biofilm thickness in cm; nB is the number of divisions in biofilm phase; R_Bn is the biological reaction rate of n compound in mg $L^{-1}\ s^{-1}$ (see Equations 7 and 8 for more details).

Biological kinetics expressions.

Aerobic heterotrophic bacteria use oxygen (O) and glucose (G) as electron acceptor and carbon source respectively. A Monod model was used to describe the bacteria growth, limited by oxygen, considering an endogenous metabolism in absence of substrate (Equation 6). Oxygen and glucose are related to microbial growth considering glucose in excess (Equations 7 and 8). This assumption was verified experimentally, finding glucose concentration through the bioreactor far superior to $K_{S,G}$.

$$\frac{dX(i,j)}{dt} = \mu_{\max}\cdot\frac{C_BO(i,j)}{K_{S,O}+C_BO(i,j)}\cdot\frac{C_BG(i,j)}{K_{S,G}+C_BG(i,j)}\cdot X(i,j)-k_d\cdot X(i,j) \quad (6)$$

$$R_BO(i,j) = -\frac{1}{Y_{X/O}}\cdot\left[\mu_{\max}\cdot\frac{C_BO(i,j)}{K_{S,O}+C_BO(i,j)}\cdot X(i,j)+k_d\cdot X(i,j)\right] \quad (7)$$

$$R_BG(i,j) = -\frac{1}{Y_{X/G}}\cdot\left[\mu_{\max}\cdot\frac{C_BO(i,j)}{K_{S,O}+C_BO(i,j)}\cdot X(i,j)\right] \quad (8)$$

where X is the biomass concentration in g L^{-1}; μ_{max} is the maximum specific growth rate in s^{-1}; C_Bn is the concentration of n compound in the biofilm phase in mg L^{-1}; $K_{s,n}$ is the Monod half-saturation coefficient for n compound in mg L^{-1}; k_d is the maintenance factor for oxygen in s^{-1}; and $Y_{X/n}$ is the n compound-biomass yield.

Numerical Solution.

The resulting set of simultaneous ordinary differential equations was solved in MATLAB® Release 2014a, using a variable order method based on the numerical differentiation formulas (NDFs) to solve stiff differential equations. An optimal discretization of the bioreactor was found, running simulations at different discretizations and optimizing results and time computing. As a result, seven mesh points were used for discretising the reactor length, and seven nodes more to discretise the biofilm thickness.

CFD modeling

CFD model was implemented and simulated using ANSYS® Academic Research, Release 14.5 software. A single-phase model was used to characterize the bioreactor performance. The bioreactor was defined by a single domain, and the biomass was introduced as a subdomain in the lower part. The liquid phase was circulating from the inlet to the outlet of bioreactor, passing over the biomass

region, which remains immobile inside de bioreactor. The liquid phase was composed by water, glucose (feeding in excess) and oxygen at saturation concentration. A hydraulic pressure loss model was introduced in the momentum equation in order to model physical characteristics of biomass.

The implementation of biological reactions in the CFD software was performed using the methodology proposed by Climent et al. (2014). Variables of kinetic expressions where defined as additional variables (oxygen, glucose and biomass) in the domain, including an extra transport equation for each additional variable:

$$\frac{\partial(\rho\varphi)}{\partial t} + \nabla \cdot \left(\rho\, U\, \varphi\right) = \nabla \cdot \left(\rho\, D\phi\, \nabla\varphi\right) + S_{\varphi} \qquad (9)$$

where U is the fluid velocity, ρ is the mixture density (mass per unit volume), ϕ is the conserved quantity per unit volume (concentration), φ=ϕ/ρ is the conserved quantity per unit mass, S_{φ} is a volumetric source term, with units of conserved quantity per unit volume per unit time and Dϕ is the kinematic diffusivity for the variable.

All terms in Equation 9 were considered for oxygen and glucose, whereas diffusive term was neglected for the biomass additional variable. In addition, the differential equations for the kinetics biodegradation and biomass growth (Equation 6-8) were included as source terms.

During the meshing process, the guidelines detailed in *CFX Best Practices Guide for Numerical Accuracy* (ANSYS, 2012) were took into account, testing mesh dependence and discretization schemes. Then, a sensitivity analysis of the mesh was performed and the results were independent.

Finally, simulations were calculated in transient and steady state, defining in both of them a laminar flow regime. The simulation results were obtained after following two steps. First, a stationary solution for the fluid with no additional variables was calculated. Secondly, the resulting hydrodynamic variables were kept constant for the transient simulation, and only the transport equations for the additional variables were solved. Convergence was assumed when the maximum residual of each equation (momentum, mass and additional variables) reached a value less than $1 \cdot 10^{-4}$ and additional variables kept in a constant value.

RESULTS AND DISCUSSION

Comparison of mathematical and CFD model results

The bioreactor mathematical model does not consider mass transfer characteristics, consequently, a set of CFD simulations were carried out considering the same initial conditions of MATLAB® model and without any hydrodynamic effects such as turbulence modeling or mass transfer limitations (as a CSTR), in order to validate the implementation of biological expressions and fitted parameters into the CFD code. The results of simulating the bioreactor performance in MATLAB® and ANSYS® are shown in Figure 1. These simulations were carried out with fitted parameters from experimental results for the specific rates of oxygen utilisation. Moreover, an average of the experimental DO profiles, with their corresponding error bar, is shown in Figure 1. The graphs of mathematical model and CFD results show logical trends and satisfactory agreement for different biofilm densities. Thus, fitting the kinetic constants and their implementation into CFD software can be stated as successful. On the other hand, in the comparative with the experimental results, the normalized root mean square errors (NRMSE) between the experimental DO measurements and the DO simulations using CFD model for the different biofilm densities (9.3 g VSS L^{-1}, 13.5 g VSS L^{-1} and 18.2 g VSS L^{-1}) are 6.48%, 14.06% and 9.07% respectively. One should keep in mind that these simulations do not consider mass transfer phenomena. Even so, the predictions of both models have a low NRMSE and illustrate good congruency with experimental profiles at two different densities (Figure 1A and 1C).

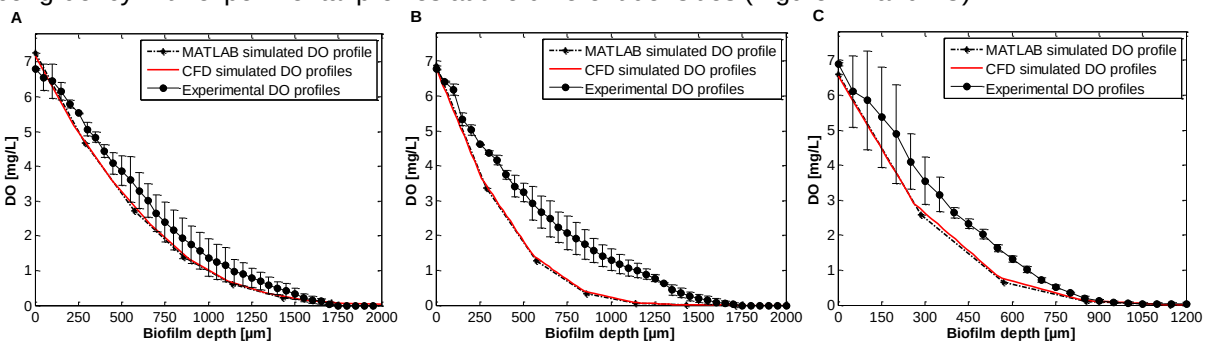

Figure 1. Simulated DO profiles (without including convective and temporal terms) and experimental DO profiles inside the biofilm under substrate consumption operating conditions at different biofilm densities: A) 9.3 g VSS L^{-1}; B) 13.5 g VSS L^{-1}; and C) 18.2 g VSS L^{-1}.

CFD simulation results

Another set of CFD simulations were carried out. An adaptive mesh refinement was considered during meshing process, and all the terms in the Equation 9 (convective, temporal and diffusive terms) were included in the definition of CFD model.

The hydrodynamics characterization of bioreactor was studied from streamlines and velocity profiles, which are shown in a front view of the FPB (Figure 2). The velocity profiles in the liquid phase of the bioreactor match quite well the velocity distribution of a laminar flow regime (Figure 2C). The streamlines (Figure 2A) show the liquid phase was correctly distributed over the bioreactor, contacting the overall of the biomass (specified in brown colour) to provide all the necessary nutrients. Moreover, the liquid phase did not have a drag effect over the biomass phase, thus biomass growth is favored by the design of the bioreactor. The velocity profiles (Figure 2B) identify bioreactor zones which support the highest and lowest velocities. The highest velocity was in the outlet section (point P4), when the fluid leaves the reactor. The bioreactor zones which supported lower velocities were mainly in the biomass domain (point P3). Therefore, diffusive phenomena were predominant over mass transport in those zones.

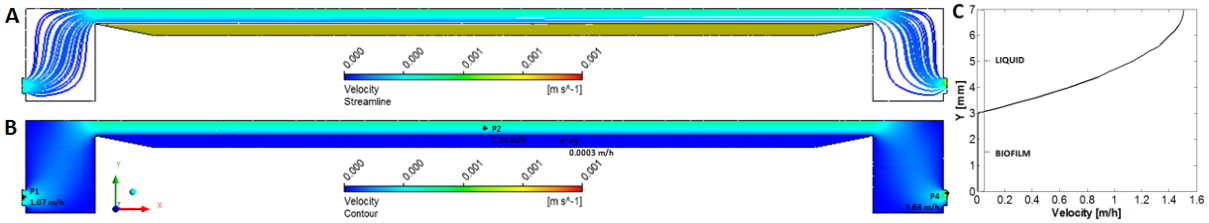

Figure 2. Velocity streamlines (A) and profiles (B) inside the bioreactor and axial velocity profile (C) in the bioreactor.

Regarding to simulated DO profiles, in contrast to other CFD studies in which simulations have been used to model de biological reactions inside de bioreactor (Feng et al., 2007; Jia et al., 2009; Wang et al., 2011), in the present work, the results of simulating DO profiles within the biofilm are shown and compared with experimental ones. Figure 3 shows the experimental and simulated DO profiles obtained at three positions along the bioreactor, corresponding to different biofilm densities. Experimental and CFD simulated profiles present the same behaviour and the same trend throughout the biofilm, reaching the anaerobic limit at similar depths, for all the studied biofilm densities. It should be noted that biofilm depth depends on biofilm density. Therefore, the CFD model represents correctly this behavior, decreasing slowly oxygen when biofilm is less dense (Figure 3A versus Figure 3C). Moreover, the NRMSE between the experimental and simulated DO profiles for the different biofilm densities (9.3 g VSS L^{-1}, 13.5 g VSS L^{-1} and 18.2 g VSS L^{-1}) are 1.17%, 6.32% and 3.53% respectively, so a good agreement has been reached using the CFD model. Hence, comparing these CFD profiles with simulated profiles from Figure 1, in which mass transfer phenomena was not considered, the fact of including convective and temporal terms in the CFD model greatly improves the simulations results, reducing the NRMSE between 5.31% and 7.74% for the studied conditions. Therefore, the developed CFD model could be used to determine the effective thickness of biofilm and to differentiate between aerobic and anaerobic zones in the biomass domain.

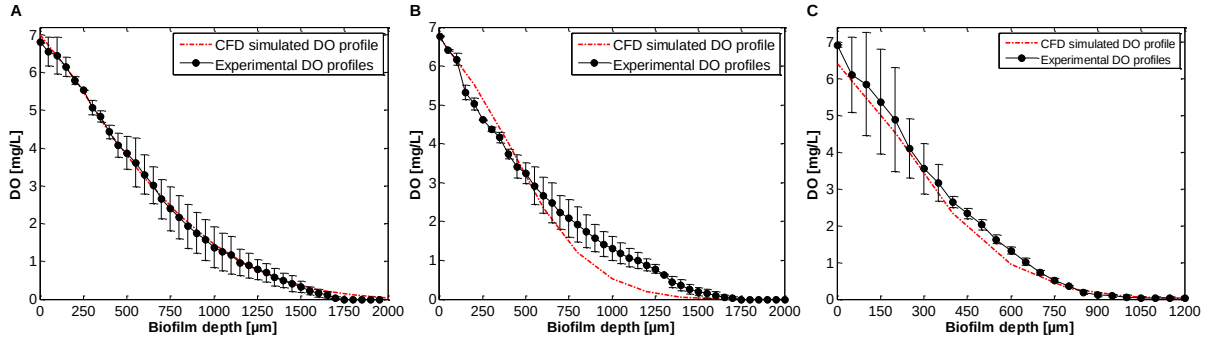

Figure 3. CFD simulated DO profiles (including convective and temporal terms) and experimental DO profiles inside the biofilm under substrate consumption operating conditions at different biofilm densities: A) 9.3 g VSS L^{-1}; B) 13.5 g VSS L^{-1}; and C) 18.2 g VSS L^{-1}.

Finally, the CFD model allows to study the behaviour of the biological kinetics expressions in the length of the bioreactor. As can be seen in a top view of the FPB, CFD model reproduces correctly oxygen and glucose degradation (Figure 4A and 4B), decreasing their concentrations along the

bioreactor. Conversely, the biomass profile (Figure 4C) increases its concentration across the length of the FPB, as a result of combining the hydraulic effect over the biomass and growing kinetics.

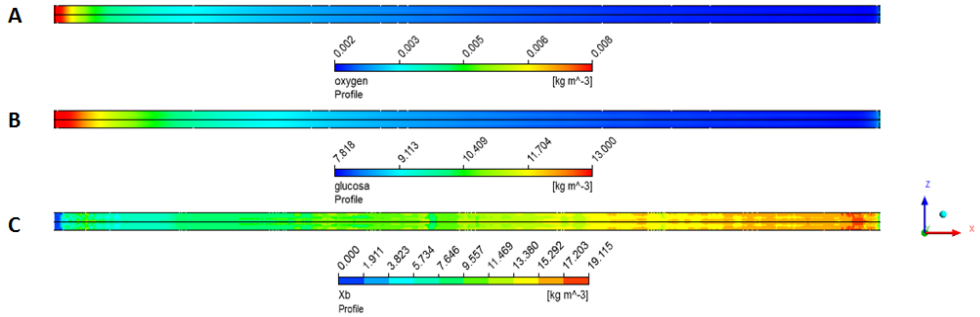

Figure 4. Oxygen (A) and (B) glucose degradation profile along the bioreactor, and biomass concentration profile along the bioreactor (C).

CONCLUSIONS

In the present work, metabolic activity in the FPB has been studied recording experimental DO profiles and developing a mathematical model to describe mass transport and biological reactions. Then, a detailed model of the bioreactor was been developed using CFD software, implementing the biokinetics expressions into the code as transport equations. Convective, temporal and diffusive terms were included in order to properly reproduce biofilm behavior. These differential equations were solved at each time step, coupling them with the hydrodynamic characterization. Therefore, a CFD model was developed and solved to simulate local transient flow and dynamic behavior of biofilm growth and glucose biodregradation in the FPB. The CFD simulation results were validated comparing simulated DO profiles and experimental DO profiles within the biofilm section. The simulated DO profiles illustrate a satisfactory agreement with experimental data. In addition, a first approach regarding the application of CFD tool to the simulation of biochemical reactions in biofiltration systems has been tested, obtaining succesful results. With this novel tool, the spatial and temporal behavior of biological systems coupled with hydrodynamics effects could be studied in detail, being the key to optimize the performance of this type of bioreactors.

As future work, the CFD model will be refined including the gas-phase, where the pollutant will be supplied to the reactor.

ACKNOWLEDGEMENTS

This work has been founded by the project CTM2012-37927-C03-02, financed by the Ministerio de Economía y Competitividad (Spain). Lledó Prades gratefully acknowledges a FPI-2013 predoctoral scholarship, and Xavier Guimerà also acknowledges a FPI-UPC predoctoral scholarship, from Ministerio de Economía y Competitividad and Universitat Politècnica de Catalunya respectively.

References

ANSYS, Inc. *ANSYS CFX Reference Guide, ANSYS CFX Release 14.5*, A. Inc., Ed., Canonsburg (2012) 81–99.
Bradford, M. M. *Analytical Biochemistry 72*(1-2) (1976) 248–254.
Climent, J., Martínez-Cuenca, R., Berlanga, J. G., Julián-López, B., Chiva, S. World Water Congress & Exhibition (IWA 2014) Proceedings, IWA (Ed.), Lisbon (2014).
Dorado, A. D., Baquerizo, G., Maestre, J. P., Gamisans, X., Gabriel, D., Lafuente, J. *Chemical Engineering Journal* 140 (2008) 52–61.
Feng, W., Wen, J., Liu, C., Yuan, Q., Jia, X., Sun, Y. *Biotechnology and Bioengineering 97*(2) (2007) 251–264.
Guimerà, X., Moya, A., Dorado, A. D., Villa, R., Gabriel, D., Gabriel, G., Gamisans, X. *Applied Microbiology and Biotechnology* 99(1) (2015) 55-66.
Iranpour, R., Cox, H. H. J., Deshusses, M. A., Schroeder, E. D. *Environmental Progress 24*(3) (2005) 254–267.
IWA Task Group on Biofilm Modeling (Eds.). Mathematical Modeling of Biofilms, Report 18, IWA Task Group on Biofilm Modeling, Scientific and Technical IWA Publishing, London (2006) 25-30.
Jia, X., Wen, J., Wang, X., Feng, W., Jiang, Y. *Industrial & Engineering Chemistry Research 48*(9) (2009) 4514–4529.
Kim, S., Deshusses, M. A. *Environmental Progress* 22(2) (2003) 119–128.
Lewandowski, Z., Beyenal, H. Fundamentals of biofilm research, L. Taylor & Francis Group, Ed., Boca Raton (2007) 452.
Liotta, F., Chatellier, P., Esposito, G., Fabbricino, M., Van Hullebusch, E. D., Lens, P. N. L. *Critical Reviews in Environmental Science and Technology 44*(23) (2014) 2642–2673.
Nguyen, M. T., Appan, A., Tan, D. S., Tan, S. K. *Journal of Environmental Engineering 140*(3) (2014) 1-7.
Perry, R. H., Green, D. W. Perry's chemical engineer's handbook (7th editio.), Mc Graw-Hill (1997).
Picioreanu, C., Loosdrecht, M. C. M. Van, Heijnen, J. J. *Biotechnology and bioengineering* 68(4) (2000) 355-369.
Picioreanu, C., Loosdrecht, M. C. M. Van, Heijnen, J. J. *Biotechnology and bioengineering* 72(2) (2001) 205-218.
Stewart, P. S. *Biofouling 28*(2) (2012) 187–98.
Taherzadeh, D., Picioreanu, C., Küttler, U., Simone, A., Wall, W. A, Horn, H. *Biotechnology and Bioengineering 105*(3) (2010) 600–10.
Wang, X., Jia, X., Wen, J. *Chemical Engineering Journal 172*(2-3) (2011) 735–745.